Soft Matter

RSC Publishing

PAPER

View Article Online
View Journal | View Issue

Cite this: *Soft Matter*, 2013, **9**, 8678

Kinetics of chitosan hydrogel formation in high internal phase oil-in-water emulsions (HIPEs) using viscoelastic measurements

Jonathan Miras,[a] Susana Vílchez,[a] Conxita Solans,[a] Tharwat Tadros[b] and Jordi Esquena*[a]

High internal phase emulsions (HIPEs) have been used as templates for the preparation of low-density highly porous chitosan foams. The formation of hydrogels and porous foams, by crosslinking in the external phase of O/W HIPEs, has been studied. The stability of the emulsions, prepared using a nonionic surfactant (C13/C15 alkyl chains with 7 moles ethylene oxide), was investigated using droplet size *vs.* time measurements, in the presence and absence of chitosan. The stability was also assessed using dynamic (oscillating) measurements, where the storage modulus (G'_{LVR}) and cohesive energy density (E_c) were measured as a function of time. The effect of agitation was investigated by preparing the HIPEs at 700, 900 and 1200 rpm. The HIPEs prepared using nonionic surfactants in the absence of chitosan gave large droplet sizes but they were quite stable against coalescence. Addition of chitosan caused a significant reduction in droplet size and polydispersity, but the emulsions were less stable against coalescence. For emulsions prepared at low speeds of agitation (700 and 900 rpm), both G'_{LVR} and E_c showed an initial increase of the modulus due to flocculation, but at times longer than 24 h, the flocculated emulsion showed coalescence. In the presence of chitosan, all HIPEs showed an exponential decrease in G'_{LVR} and E_c with time, indicating coalescence of the emulsion. The crosslinking of chitosan with genipin was investigated using oscillatory and creep measurements. Both methods showed an increase in G'_{LVR}, E_c and compliance J with time, reaching a plateau value when $t \geq 24$ h. This clearly shows completion of the crosslinking process after 24 h. Finally, crosslinked chitosan porous foams were obtained and characterized by SEM, which showed uniform porous textures.

Received 16th May 2013
Accepted 18th July 2013

DOI: 10.1039/c3sm51375k

www.rsc.org/softmatter

Introduction

During the last two decades, polymeric hydrogels have been intensively studied due to their potential applications in a variety of fields, such as chemical engineering, biotechnology and pharmaceuticals.[1–4] Hydrogels can change their characteristics, in particular swelling, as a result of changes in the external environment such as pH, temperature, ionic strength or application of an electric current.[5–8] Hydrogels can be potentially applied as drug delivery systems. For this purpose, it is necessary to use biocompatible and biodegradable polymers. The drugs can be incorporated into the hydrogel matrix and by changing the conditions, such as pH, temperature or ionic strength, a controlled release can be achieved.

The preparation methods by direct crosslinking in aqueous media to obtain chitosan hydrogels do not allow one to control porosity and pore size distribution in such materials. We have recently developed a new procedure to synthesize chitosan porous materials by a simple single-step method which provides a direct route to obtain these chitosan foams.[9] This procedure, as mentioned above, involves crosslinking with a low toxicity reagent, genipin, in the external phase of oil-in-water (O/W) highly concentrated emulsions. Since emulsions are thermodynamically unstable, several breakdown processes occur with time through different instability mechanisms, *e.g.*, flocculation, coalescence and Ostwald ripening.[10]

Emulsion-templating techniques are versatile for the preparation of well-defined and controlled porous organic polymers,[11–15] inorganic materials[16–19] and inorganic–organic composites.[20,21] The technique involves the preparation of high internal phase emulsions (HIPEs), which has a volume fraction of the dispersed phase (ϕ) larger than the theoretical maximum packing volume fraction ($\phi = 0.74$) for equal size spheres. When $\phi > 0.74$, the droplets loose the spherical shape and take the form of a polyhedron,[22–24] similar to the structure of a foam. After polymerization/crosslinking in the continuous phase of the highly concentrated emulsion, the dispersed phase (emulsion droplets) is removed to give rise to a porous replica material of the emulsion.[9,24–29]

[a]*Institute for Advanced Chemistry of Catalonia, Consejo Superior de Investigaciones Científicas (IQAC-CSIC) and CIBER de Bioingeniería, Biomateriales y Nanomedicina (CIBER-BBN), Jordi Girona 18-26, Barcelona, Spain. E-mail: jordi.esquena@iqac.csic.es; Fax: +34 93 204 59 04; Tel: +34 93 400 61 78*

[b]*89 Nash Grove Lane, Wokingham, Berkshire RG40 4HE, UK*

In the present paper, we have investigated the stability of high internal phase emulsions (HIPEs) used as templates, by measuring the droplet size and viscoelastic properties as a function of time. The crosslinking reaction of chitosan in highly concentrated oil-in-water emulsions was also investigated using viscoelastic measurements. Porous chitosan foams were obtained after crosslinking and solvent removal. Finally, the topography of chitosan foams was characterized. The capacity of this emulsion-templating technique to tailor the foam pore size, by controlling the emulsion droplet size, was evaluated.

Chitosan is the most commonly used cationic naturally occurring polysaccharide that can be applied in drug delivery systems due to its biocompatibility, biodegradability, non-toxic nature and film-forming properties.[8,30–34] Chitosan is obtained by alkaline deacetylation of chitin, which is the principal component of the protective skeleton of crustaceans (such as crabs and shrimps) and of the cell walls of some fungi.[35] Chitin and chitosan are formed by units of *N*-acetyl-D-glucosamine and D-glucosamine, joined by β-[1 → 4] links. When the D-glucosamine ratio is higher than 60%, the final product is called chitosan.[32] Chitosan has a $pK_a \approx 6.5$, and it becomes positively charged when the pH is less than 6. Under these conditions, the molecule becomes water soluble.[8,30,36]

Different crosslinkers can be used to crosslink chitosan through the reaction with amino groups, such as glutaraldehyde, formaldehyde or epoxy compounds.[37–39] The present investigation is focused on the use of a natural crosslinker reagent, namely genipin (obtained from the fruits of *Gardenia jasminoides* ELLIS), since it is 5000–10 000 times less cytotoxic than glutaraldehyde.[40]

The main objective of the current study is to investigate the formation of hydrogels and porous foams, by templating in high internal phase emulsions (HIPEs). For this purpose, rheological properties and droplet size determinations, as a function of time, have been studied, which can provide useful information on the physical stability of the emulsions. The influence of the presence of chitosan in the continuous phase of emulsions is evaluated since chitosan could affect the stability of emulsions, as described before.[41–43] Another important objective is to achieve an appropriate control of emulsion droplet size, allowing us to obtain the desired pore size of the chitosan final porous foams.

Furthermore, the chitosan crosslinking process and its kinetics, produced in the continuous phase of emulsions to obtain chitosan hydrogels, are also studied by rheological measurements. Finally, the topography of crosslinked chitosan foams was characterized to evaluate the structure of foams.

Materials and methods

Materials

Chitosan (medium molecular weight, $M_w \approx 300$ kDa) with 85% deacetylation degree was purchased from Sigma-Aldrich. The emulsifier used was a nonionic surfactant, Synperonic A7, consisting of C_{13-15} alkyl chains and 7 moles of ethylene oxides (EO), with a hydrophilic–lipophilic balance (HLB) of 12.2, and was supplied by Uniqema (UK). Decane, with 94% purity, was obtained from Fluka. The crosslinker genipin, with an average molecular weight of 226 g mol^{-1}, was obtained from Challenge Bioproducts Co. (Taiwan). Acetic acid glacial, CH_3COOH, was obtained from Panreac (Spain) with a purity of 99.5%. Deionized and filtered water and phosphate buffer solution (pH = 7.4) were used for the preparation of all solutions.

Methods

Chitosan solution at 0.02 g mL^{-1} was prepared by dissolving chitosan powder in an acetic acid solution at 1 vol% by stirring overnight (magnetic stirrer). Genipin solution was prepared at 1 wt% in phosphate buffer solution at pH = 7.4 and stirred for 1 h.

Preparation of O/W high internal phase emulsions (HIPEs)

Three different series of high internal phase oil-in-water (O/W) emulsions (HIPE1, HIPE2 and HIPE3) were prepared by dropwise addition of the dispersed phase, decane (keeping the volume fraction constant at $\phi = 0.8$), to the continuous phase at 25 °C with mechanical stirring at three different agitation rates for every series: 700, 900 and 1200 rpm. This study was carried out as a function of the continuous phase composition (Table 1). Emulsions with composition HIPE3, in the presence of a crosslinker, were used for the preparation of chitosan porous foams. For this purpose, emulsion HIPE3 was kept for 72 h in a water bath at 40 °C, as described before.[9] The resulting material was purified by Soxhlet extraction with ethanol and water for 12 h in each solvent. Finally, crosslinked chitosan foams were obtained by freeze-drying.

Droplet size measurements

The droplet size distributions were obtained after increasing the temperature from 25 to 40 °C, using optical microscopy. Emulsions were observed with a Reichert Polyvar 2 microscope, supplied by Leica (Germany), equipped with a video camera (Sony CCD-Iris). A drop of the concentrated emulsion was placed on a glass slide and optical micrographs were taken. Images were processed using the IM500 software supplied by Leica. Droplet size and size distributions were obtained from optical micrographs by sizing 800 randomly droplets, acquired using an oil-immersion objective (×100 magnification). An image analysis software program (Image J) was used for statistical analysis to calculate the droplet size distributions (expressed in vol%). From these distributions, the de Brouckere

Table 1 Composition of the continuous phase (wt%) of high internal phase emulsions

	Content, wt%		
Component	HIPE1	HIPE2	HIPE3
Synperonic A7	10	10	10
CH_3COOH 1 vol%	45	0	0
Chitosan solution 0.02 g mL^{-1}	0	45	45
Phosphate buffer pH = 7.4	45	45	0
Genipin solution 1 wt%	0	0	45

mean diameter (eqn (1)), $D[4,3]$, and the polydispersity, expressed as Span (eqn (2)), were calculated.

$$D[4,3] = \sum d^4 \Big/ \sum d^3 \quad (1)$$

where d is the droplet diameter (μm).

$$\text{Span} = \frac{d(0.9) - d(0.1)}{d(0.5)} \quad (2)$$

where $d(0.1)$, $d(0.5)$ and $d(0.9)$ are the cumulative volume distributions at 10%, 50% and 90%, respectively.

The droplet sizes of HIPE1 (with no chitosan) and HIPE2 series, with chitosan (Table 1), prepared at three agitation rates (700, 900 and 1200 rpm) were measured over 72 h at 40 °C in order to evaluate their stability.

Interfacial tension experiments

Measurements were carried out by forming a drop of surfactant (Synperonic A7) aqueous solution inside the oil (decane). These experiments were performed as a function of Synperonic A7 concentration with a syringe of 1 mL (Hamilton, Switzerland) attached into a graduated micrometer in order to achieve an accurate volume of the drop. It has to be mentioned that the manipulation of the micrometer screw must be carried out carefully to attain adsorption equilibrium. The measurement finishes when the drop is released from the needle, and its volume can be calculated by comparing the final and the starting point in the micrometer readable scale.

Crosslinking of chitosan in the HIPEs

Emulsions from the HIPE3 series (Table 1), in the presence of chitosan and crosslinker (genipin), were kept in a water bath for 72 h at 40 °C, allowing the chitosan crosslinking reaction.

Rheological measurements

These measurements were carried out using an AR-G2 controlled stress rheometer (TA Instruments). The viscosity of the continuous phase of the emulsions HIPE1 and HIPE2 (see Table 1) was measured using a steady state procedure at 25 °C with a cone-plate geometry with a diameter of 40 mm, a cone angle of 4° and a gap of 105 μm. For comparison, the viscosity of water was measured using concentric cylinders (gap = 4000 μm).

For the highly concentrated emulsions, only viscoelastic measurements were carried out using a parallel plate geometry with a diameter of 20 mm. Measurements were carried out at 40 °C for 72 h with a solvent trap, to avoid evaporation. Two types of viscoelastic measurements were performed, namely oscillating and creep measurements. In the oscillating technique, a sinusoidal strain with amplitude (γ_0) is applied on the system and the stress amplitude (σ_0) is measured simultaneously. From the time shift (Δt) between stress and strain amplitudes and the frequency, ω (rad s^{-1}), the phase angle shift (δ) is obtained. From γ_0, σ_0 and δ, the following rheological parameters are estimated: complex modulus (eqn (3)), storage or elastic modulus (eqn (4)) and loss or viscous modulus (eqn (5)).

$$|G^*| = \sigma_0/\gamma_0 \quad (3)$$

$$G' = |G^*| \cdot \cos\delta \quad (4)$$

$$G'' = |G^*| \cdot \sin\delta \quad (5)$$

The elastic modulus values were taken in the linear viscoelastic region (G'_{LVR}), which are independent of the applied strain. For this purpose, the strain was gradually increased, from 0.01 to 20% for emulsions HIPE1 and from 0.05 to 20% for HIPE2, both at a frequency of 1 Hz and a gap of 1000 μm. For the evaluation of the crosslinking process, two types of measurements were carried out for emulsions HIPE3 as a function of time. In the first experiment, the elastic modulus in the linear viscoelastic region (G'_{LVR}), at a frequency of 2 Hz, was measured as a function of time for 72 h. In the second experiment, creep measurements were carried out at constant shear stresses of 10 and 40 Pa and the variation of the compliance J ($J = \gamma/\sigma$), determined in the linear viscoelastic region, was obtained with time, where γ is the deformation and σ the applied stress. Measurements were also carried out for 2 min after removing the stress (creep recovery). These creep and recovery measurements were performed as a function of time (0, 2, 4, 6, 24, 48 and 72 h). In these kinetics measurements, the gap of the parallel plate geometry was kept at 2700 μm. This characterization has been performed by the Nanostructured Liquid Characterization Unit of the Spanish National Research Council (CSIC) and the Biomedical Networking Center (CIBER-BBN), located at IQAC-CSIC.

Surface characterization of crosslinked chitosan foams

Crosslinked chitosan porous foams, obtained by the emulsion-templating technique at 700, 900 and 1200 rpm, were characterized by Scanning Electron Microscopy (SEM). A Hitachi 4100 microscope was used, operating at 15 kV. Samples were previously coated with gold by sputtering.

Results and discussion

Stability of the high internal phase emulsions (HIPEs), in the presence and absence of chitosan, using droplet size measurements

Table 2 shows the average droplet size diameter, $D[4,3]$, and the polydispersity, Span, of the emulsion HIPE1 without chitosan, as a function of time at three different speeds of agitation.

The above results show a systematic reduction in drop size with increase of agitation rate, as expected. Also, the average

Table 2 Average droplet diameter, $D[4,3]$ (μm), and polydispersity, Span, for HIPE1 (without chitosan) as a function of agitation rate and time

	$t = 0$ h		$t = 24$ h		$t = 48$ h		$t = 72$ h	
	$D[4,3]$	Span	$D[4,3]$	Span	$D[4,3]$	Span	$D[4,3]$	Span
700 rpm	5.2	0.9	5.5	0.9	6.4	0.8	6.5	0.8
900 rpm	3.5	1.1	4.1	0.9	4.2	0.8	4.3	0.9
1200 rpm	2.1	0.9	2.3	0.8	2.4	0.8	2.7	0.9

size increases slightly with increase of time, whereas Span remains almost constant. The slight increase of the average droplet size with time could be the result of coalescence and/or Ostwald ripening.[44]

To test which one of these processes is the main cause of instability, we have plotted cubic radius (r^3) *vs.* time for Ostwald ripening.[45,46] However, the plots of r^3 *vs.* time (data not shown) did not show a linear fit, at any agitation speed. Therefore, most likely, the instability is not produced by Ostwald ripening, and it could be attributed to coalescence.

Different models could be used to evaluate if coalescence was the main instability process. The coalescence rate could be quantified using the Deminiere model,[47] which explains the formation of critical holes between adjacent droplets, leading to the rupture of stabilizing films and producing coalescence. This process may be described by eqn (6), which was applied to rather monodisperse and concentrated emulsions.[47]

$$1/r^2 = 1/r_0^2 - (3\pi/8)\omega t \quad (6)$$

where r is the droplet radius at time t, r_0 is the initial droplet radius and ω is the frequency of rupture per unit surface of the film. However, in the present case, the Deminiere model did not produce an acceptable linear fit to the experimental results (data not shown).

Assuming that the coalescence rate may have a first order kinetics, certainly governed by the rupture of the aqueous film that separates adjacent droplets,[48–50] the droplet size could follow:

$$\log r = \log r_0 + kt \quad (7)$$

where r is the droplet radius at time t, r_0 is the value at $t = 0$ and k is the coalescence rate. In the present case, plots of logarithm of droplet radius *vs.* time show linear fits that are reasonably good (Fig. 1). Consequently, the instability process is probably dominated by coalescence, which follows a first order kinetics.

From these fits, the coalescence rate was calculated from the slopes, obtaining a fairly constant value, between 0.0012 and 0.0015 h^{-1}, which is very low indicating reasonable stability for the emulsions. Addition of chitosan in the continuous phase (HIPE2) showed a significant reduction in the average droplet diameter at all agitation speeds (Table 3). This could be due to the increase of the viscosity of the continuous phase which results in an increase in stress produced during agitation (the stress is given by the product of velocity gradient and the viscosity).[51] However, these emulsions were less stable than those obtained in the absence of chitosan, showing higher coalescence rates (ranging from 0.0036 to 0.0052 h^{-1} depending on the agitation rate) as indicated in Fig. 2 (plots of droplet radius *vs.* time).

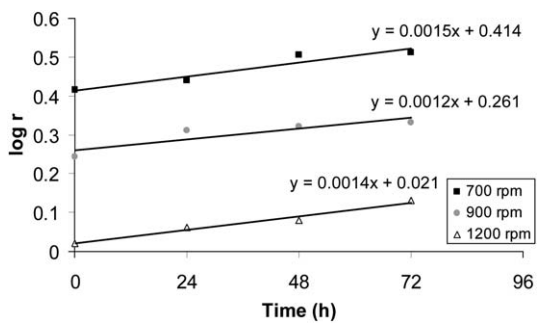

Fig. 1 Logarithm of droplet radius *vs.* time for HIPE1 (without chitosan).

Table 3 Average droplet diameter, $D[4,3]$ (μm), and polydispersity, Span, for HIPE2 (with chitosan) as a function of agitation rate and time

	$t = 0$ h		$t = 24$ h		$t = 48$ h		$t = 72$ h	
	$D[4,3]$	Span	$D[4,3]$	Span	$D[4,3]$	Span	$D[4,3]$	Span
700 rpm	1.5	0.7	2.1	0.6	2.2	0.7	3.5	1.0
900 rpm	1.4	0.8	1.9	0.7	2.2	0.8	2.6	0.8
1200 rpm	0.9	0.5	1.2	0.6	1.7	0.7	2.1	0.7

On addition of chitosan, the interfacial tension increases, as shown in Fig. 3. Chitosan is a polysaccharide with amino groups and hydroxyl groups. This molecule probably possesses certain amphiphilic character, being able to adsorb on interfaces and interacting with other amphiphilic compounds. At relatively low pH (below the pK_a, of chitosan, 6.5), amino groups are protonated (NH_3^+), which enhances the chitosan hydrophilic character, producing an increase in interfacial tension, leading to faster coalescence rate of emulsion droplets.[41,52]

Stability of the HIPEs using rheological measurements

Fig. 4 shows the viscosity shear stress curves for water, 10% Synperonic aqueous solution (continuous phase of HIPE1),

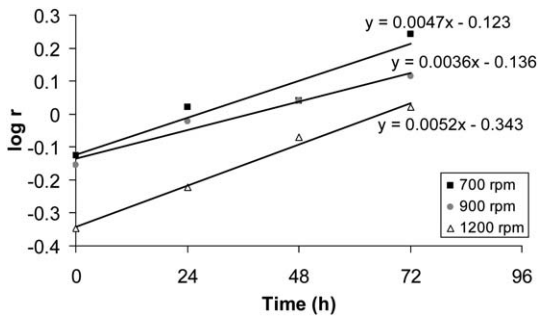

Fig. 2 Droplet radius *vs.* time for HIPE2, with chitosan.

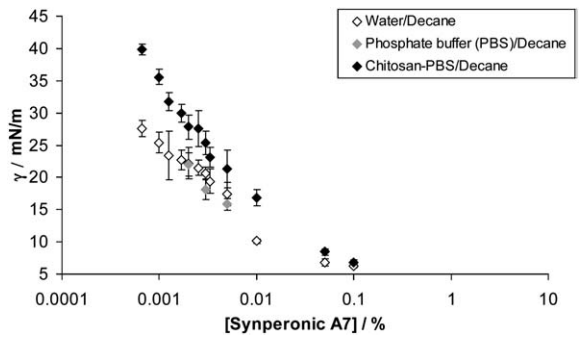

Fig. 3 Interfacial tension for the systems water/decane, phosphate buffer/decane and chitosan-phosphate buffer/decane.

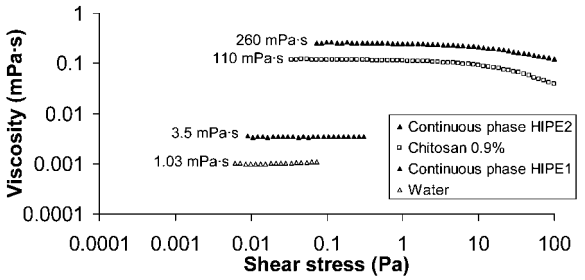

Fig. 4 Steady state measurements for water, 10% Synperonic A7 (continuous phase of HIPE1), 0.9% chitosan and 0.9% chitosan with 10% Synperonic A7 and phosphate buffer (continuous phase of HIPE2).

0.9% chitosan solution and 10% Synperonic A7/0.9% chitosan solution/phosphate buffer (continuous phase of HIPE2). Both water and 10% Synperonic A7 solution show Newtonian behavior. Addition of 10% Synperonic A7 causes a slight increase in the viscosity from 1.03 to 3.5 mPas. Both solutions of 0.9% of chitosan as well as 10% Synperonic A7/0.9% chitosan/phosphate buffer show non-Newtonian behavior, with a reduction in viscosity as the shear stress increases above 5 Pa. The 0.9% chitosan solution has a much higher viscosity (110 mPas) when compared with that of the 10% Synperonic A7 solution. Addition of 10% Synperonic A7 to chitosan solution causes a high increase of the viscosity (260 mPa s). This illustrates the interaction between Synperonic A7 and the chitosan molecule as discussed in the previous section.

The stability of the emulsions is determined by following the storage modulus (in the linear viscoelastic region) as a function of time for the two systems, HIPE1 and HIPE2, at three speeds of agitation (Fig. 5).

Fig. 5A shows the results for HIPE1 (absence of chitosan). The emulsion prepared at low speed (700 rpm) shows an initial increase in the modulus for 48 h, after which it decreases from 48 to 72 h. The initial increase in the modulus may be due to flocculation since in this case the droplets are quite large ($D[4,3] = 5.2$ μm).[52] The flocculated emulsion finally undergoes some coalescence at longer periods of time. The emulsion prepared at 900 rpm shows only a small reduction of G'_{LVR} during the period from $t = 0$ h to 72 h. This shows the high stability of the emulsion as inferred from Fig. 1. The emulsion prepared at 1200 rpm shows the expected exponential decrease of G'_{LVR} *vs.* time, which indicates the presence of coalescence that produces an increase in droplet size.[53,54] The results obtained in the presence of chitosan (Fig. 5B) all show an exponential decrease of G'_{LVR} *vs.* time at all rotational speeds. These rheological results are consistent with the results obtained using droplet size measurements (Fig. 2) which show high coalescence rates (0.0036–0.0052 h^{-1}) when compared to the results obtained in the absence of chitosan.

An alternative method to measure the stability is to follow the variation of cohesive energy density of the emulsion (E_c, eqn (8)) as a function of time.[55]

$$E_C = \frac{1}{2} G'_{LVR} \gamma_{cr}^2 \quad (8)$$

where G'_{LVR} (Pa) is the storage modulus in the linear viscoelastic region and γ_{cr} is the critical strain above which non-linear response is obtained where G' decreases with increase of strain amplitude. The cohesive energy density is a useful quantitative

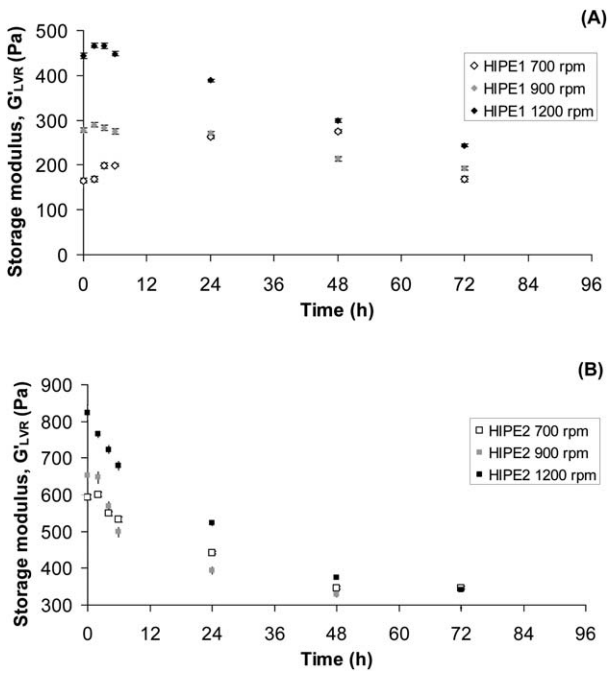

Fig. 5 Storage modulus values in the linear region, G'_{LVR}, as a function of time for HIPE1, in the absence of chitosan (A), and for HIPE2, in the presence of chitosan (B), at 700, 900 and 1200 rpm. All measurements were carried out at a frequency of 1 Hz.

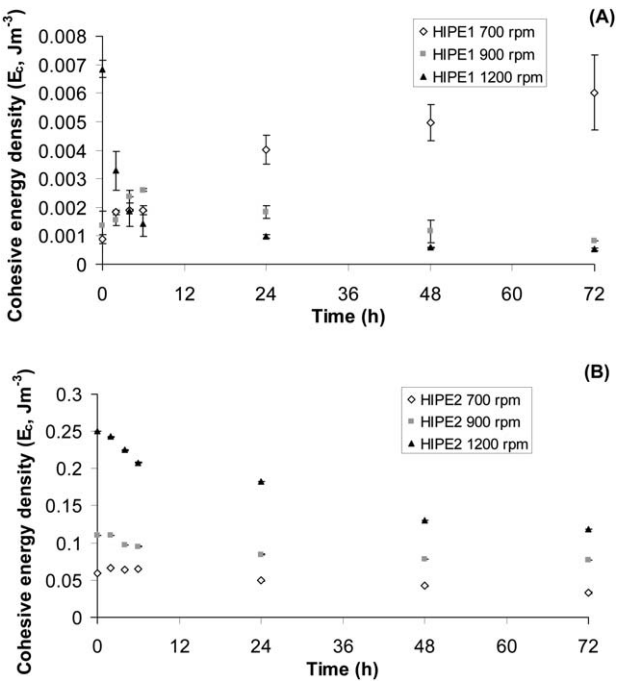

Fig. 6 Cohesive energy density values, E_c, as a function of time for HIPE1, in the absence of chitosan (A), and for HIPE2, in the presence of chitosan (B), prepared at 700, 900 and 1200 rpm.

parameter to measure the structure strength of an emulsion. The cohesive energy density depends on the droplet size distribution and the interaction forces between droplets.

The emulsion prepared at 700 rpm shows an increase in E_c with time, which indicates possible flocculation of the emulsion droplets due to attractive interactions between droplets (Fig. 6A). The emulsions prepared at 900 rpm do not show a significant change in E_c with time, indicating the emulsion stability. However, emulsions prepared at 1200 rpm show an exponential decrease of E_c with time, indicating some emulsion coalescence. The reduction of the number of contacts between droplets, produced by the increase of droplet size, causes a reduction in E_c.[50] The emulsions prepared in the presence of chitosan, HIPE2 (Fig. 6B), also show a small change in E_c with time when the stirring speed was relatively low (700 and 900 rpm). However, the emulsions prepared at 1200 rpm show the expected exponential decrease of E_c *vs.* time and this reflects the higher rate of coalescence (See Fig. 2).

Investigation of the crosslinking process

The kinetics of the crosslinking process was carried out by following the variation of elastic modulus, G'_{LVR} (in the linear viscoelastic region at a frequency of 2 Hz), as a function of time for emulsion HIPE3, containing the crosslinker genipin. The gelation or crosslinking process has been widely studied in bulk hydrogels by rheological measurements as a function of time or temperature.[56–58] When gelation occurs, an increase of storage modulus is observed. A similar procedure was carried out to study the crosslinking of chitosan hydrogels obtained using highly concentrated emulsions as templates. The results are shown in Fig. 7 for three emulsions prepared at different agitation speeds.

The results show a logarithmic increase in G'_{LVR} with time, and it seems that a plateau is almost reached after 24 h, indicating completion of the crosslinking reaction. However, with the emulsions at 1200 rpm there is some reduction in the storage modulus between 48 and 72 h, which may be due to the shrinkage of the gel.

Fig. 8 shows the variation of cohesive energy density as a function of time for emulsions HIPE3, prepared at the same agitation speeds. The trends are similar to those of the storage modulus *vs.* time (Fig. 7).

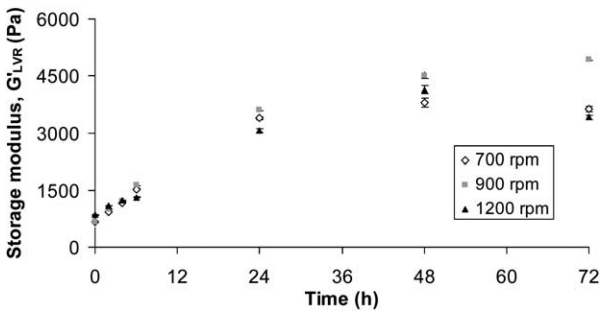

Fig. 7 Storage modulus in the linear viscoelastic region, G'_{LVR}, as a function of time for HIPE3 (with chitosan and genipin) at 700, 900 and 1200 rpm from the oscillatory strain measurements. All measurements were carried out at a frequency of 2 Hz.

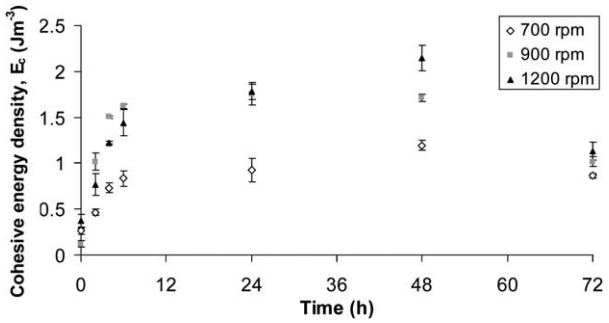

Fig. 8 Cohesive energy density, E_c, as a function of time for HIPE3 (with chitosan and genipin) at 700, 900 and 1200 rpm, obtained from oscillatory strain measurements.

Another rheological technique that can be applied to investigate the crosslinking or gelation process is constant stress (creep) measurements.[59,60] Fig. 9 and 10 show the creep compliance and recovery curves obtained at stresses of 10 Pa

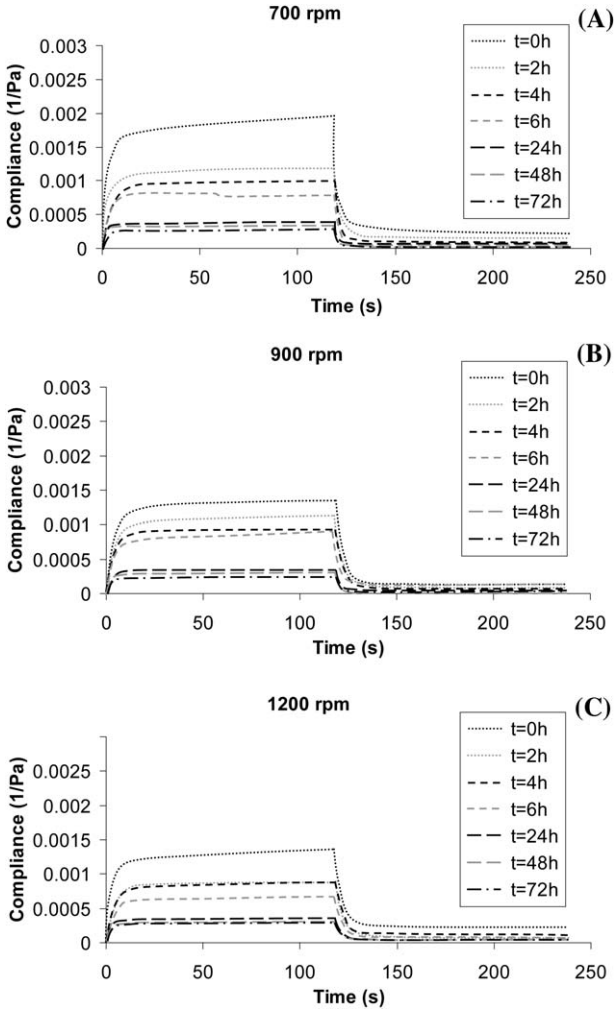

Fig. 9 Creep and recovery measurements for an applied shear stress of 10 Pa for HIPE3 emulsions prepared at 700 (A), 900 (B) and 1200 rpm (C).

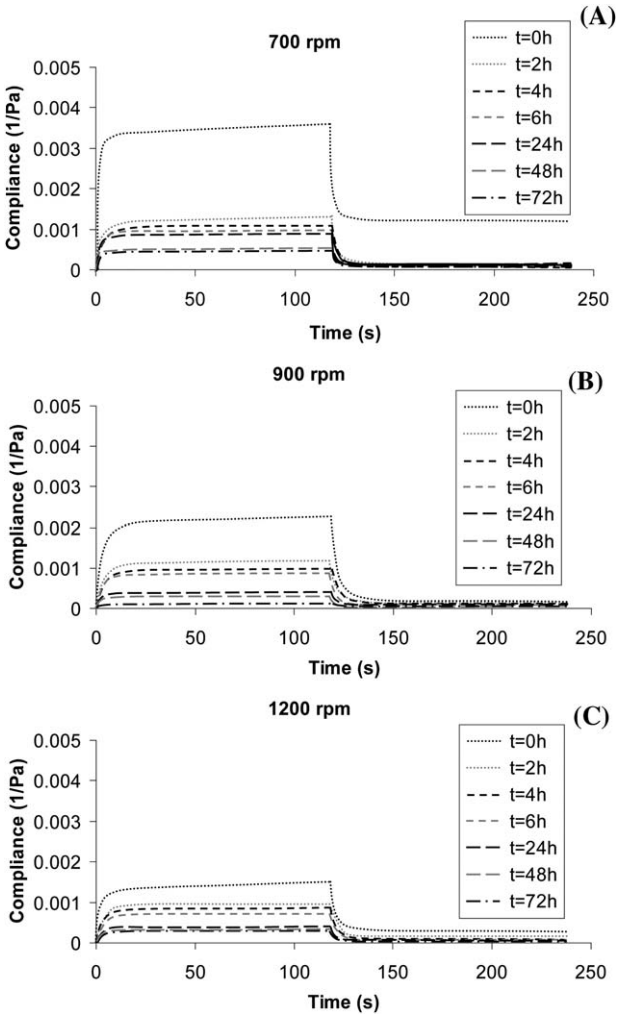

Fig. 10 Creep and recovery measurements for an applied shear stress of 40 Pa for HIPE3 emulsions prepared at 700 (A), 900 (B) and 1200 rpm (C).

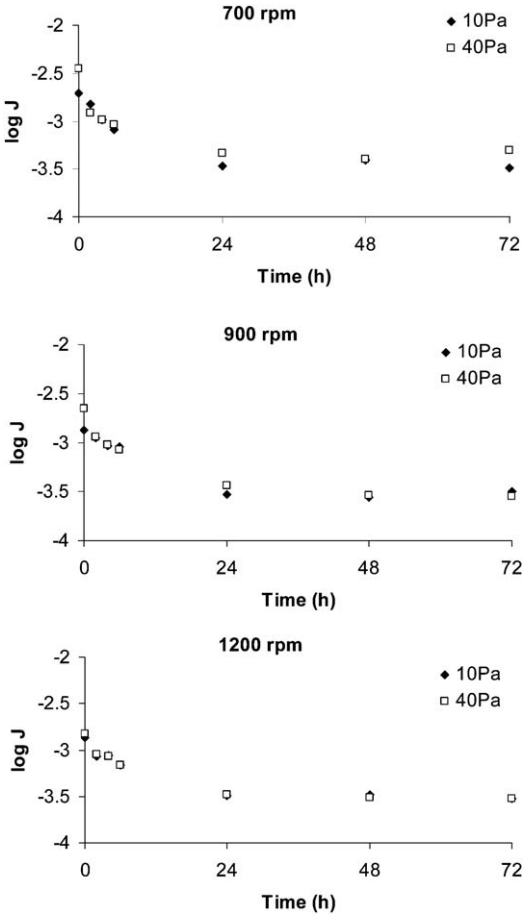

Fig. 11 Variation of log *J vs.* time at a shear stress of 10 and 40 Pa for emulsions prepared at 700, 900 and 1200 rpm.

(Fig. 9) and 40 Pa (Fig. 10) as a function of crosslinking time (0, 2, 4, 6, 24, 48 and 72 h) and for HIPEs prepared at three speeds (700, 900 and 1200 rpm). These creep curves should give clear indication of the crosslinking reaction. For example, for HIPE3 prepared at 700 rpm and $t = 0$ h (Fig. 9A) the creep curve initially shows a rapid increase in the compliance (characterized by an instantaneous compliance, J_0) followed by a slow increase in the compliance (the retarded region) and finally J shows a linear increase with increase of time, up to 120 s. When the stress is removed at this point, the compliance changes sign and the equilibrium value is reached at 240 s. The final compliance value is not equal to zero, indicating partial recovery of the structure. As the crosslinking time is increased from 0 to 72 h, the slope of the J *vs.* time curve in the initial period decreases gradually and finally it approaches 0 at $t \geq$ 24 h. In the latter cases, complete recovery is observed, indicating a change from viscoelastic liquid behavior at $t = 0$ h to viscoelastic solid behavior at $t \geq 24$ h. The trends obtained for HIPEs prepared at 900 rpm (Fig. 9B) and 1200 rpm (Fig. 9C) are similar to those obtained at 700 rpm. It should be mentioned that the compliance values obtained for emulsions prepared at 900 and 1200 rpm are lower than those obtained at 700 rpm, indicating the more solid-like behavior. The trends obtained at a stress of 40 Pa are similar to those obtained at 10 Pa, with higher compliance values in the case of 40 Pa.

Fig. 11 shows the variation of log J at the beginning of the recovery curve ($t = 120$ s) *vs.* time for the two applied stresses. In all cases, log J decreases exponentially with the increase of time, reaching a plateau at $t \geq 24$ h. These results show that the crosslinking process is almost completed after 24 h, as shown from dynamic measurements.

Topography of crosslinked chitosan porous foams

The surface characterization of chitosan foams obtained using high internal phase emulsions as templates (HIPE3) was carried out by SEM. The morphology of these materials shows a uniform porous structure. For example, a SEM image of the material obtained at 1200 rpm is shown in Fig. 12.

The pore size is smaller than the corresponding emulsion droplets, probably due to shrinkage, which was visually observed during purification by Soxhlet extraction. The droplet size from the emulsions HIPE3 used as a template is 0.9 μm at $t = 0$ h (Table 3), whereas the chitosan porous foam obtained

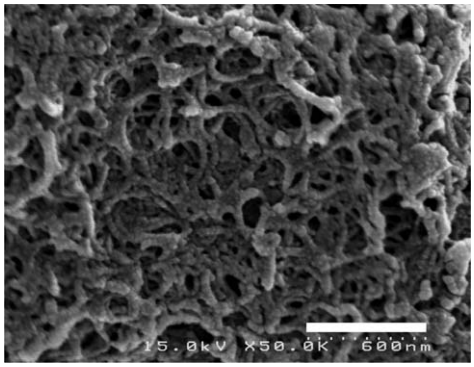

Fig. 12 SEM images of chitosan foams obtained at 1200 rpm (scale bar = 600 nm).

showed a pore size below 200 nm. Nevertheless, this templating emulsion technique allows us to obtain monolithic chitosan foams with homogeneous macropores.

Conclusions

Chitosan porous foams, with controlled pore size, were successfully obtained using oil-in-water high internal phase emulsions (HIPEs) as templates *via* chitosan crosslinking with genipin. The incorporation of chitosan produced a large decrease in droplet size, achieving emulsions with narrow droplet size distributions and with average droplet size, $D[4,3]$, below 1 μm ($t = 0$ h). Although emulsions with chitosan in the continuous phase (HIPE2) exhibited coalescence, they were suitable systems to obtain chitosan porous foams due to their narrow droplet size distributions and smaller droplet sizes. Rheological measurements showed the same trend. The influence of the agitation rate was clearly observed. By increasing the agitation rate, the storage modulus in the linear viscoelastic region (G'_{LVR}) and the cohesive energy density (E_c) increased due to the decrease of droplet size. However, both emulsions, with and without chitosan (HIPE2 and HIPE1, respectively), showed some coalescence after 6 h. The emulsions with chitosan and crosslinker (HIPE3) showed a logarithmic increase in G'_{LVR} and E_c, due to the chitosan crosslinking process, and they reached a plateau after 24 h, indicating that the crosslinking reaction is finished. The same behavior was observed by creep measurements, which reached again a plateau of compliance values after 24 h. Finally, the pore size of the porous foams was smaller than the corresponding emulsion droplets, probably due to shrinkage. However, the HIPEs proved to be useful systems for the preparation of porous chitosan foams with controlled pore size.

Acknowledgements

The authors acknowledge the Spanish Ministry of Economy and Competitiveness for the CTQ2008-06892-C03-01 and CTQ2011-23842 projects and Generalitat de Catalunya for the 2009SGR961 grant.

Notes and references

1 N. A. Peppas, K. B. Keys, M. Torres-Lugo and A. M. Lowma, *J. Controlled Release*, 1999, **62**, 81.
2 F. L. Mi, S. S. Shyu, Y. B. Wu, S. T. Lee, J. Y. Shyong and R. N. Huang, *Biomacromolecules*, 2001, **22**, 165.
3 R. A. A. Muzzarelli, P. Morganti, G. Morganti, P. Palombo, M. Palombo, G. Biagini, M. M. Belmonte, F. Giantomassi, F. Orlandi and C. Muzzarelli, *Carbohydr. Polym.*, 2007, **70**, 274.
4 J. F. Mano, *Adv. Eng. Mater.*, 2008, **10**, 515.
5 Y. M. Lee and S. H. Cho, *J. Appl. Polym. Sci.*, 1996, **62**, 301.
6 L. Brannon-Peppas and N. A. Peppas, *Chem. Eng. Sci.*, 1991, **46**, 715.
7 E. S. Gil and S. M. Hudson, *Prog. Polym. Sci.*, 2004, **29**, 1173.
8 G. Skjak-Braek, T. Anthonsen and P. Sandford, *Chitin and Chitosan*, Elsevier Applied Science, London, 1989.
9 J. Esquena, C. Solans, S. Vílchez, P. Erra and J. Miras, Spanish patent, P200930038, 2010.
10 P. Walstra, in *Encyclopedia of Emulsion Technology*, ed. P. Becher, Marcel Dekker, New York, 1983, ch. 2.
11 N. R. Cameron, D. C. Sherrington, D. C. Albistol and D. P. Gregory, *Colloid Polym. Sci.*, 1996, **274**, 592.
12 A. Barbetta, N. R. Cameron and J. S. Cooper, *Chem. Commun.*, 2000, 221.
13 J. Esquena, G. S. R. Ravi Sankar and C. Solans, *Langmuir*, 2003, **19**, 2983.
14 Z. Abbasian and M. R. Moghbeli, *J. Appl. Polym. Sci.*, 2010, **116**, 986.
15 F. Fernández-Trillo, J. C. M. van Hest, J. C. Thies, T. Michon, R. Weberskirch and N. R. Cameron, *Adv. Mater.*, 2009, **21**, 55.
16 A. Imhof and D. Pine, *Nature*, 1997, **389**, 948.
17 A. Imhof and D. Pine, *Adv. Mater.*, 1999, **11**, 311.
18 H. Maekawa, J. Esquena, S. Bishop, C. Solans and B. F. Chmelka, *Adv. Mater.*, 2003, **15**, 591.
19 Z.-Y. Yuan and B.-L. Su, *J. Mater. Chem.*, 2006, **16**, 663.
20 A. R. Mahdavian, M. Ashjari and A. B. Makoo, *Eur. Polym. J.*, 2007, **43**, 336.
21 G. Ghosh, A. Vílchez, J. Esquena and C. Solans, *Mater. Chem. Phys.*, 2011, **130**, 786.
22 K. J. Lissant, *J. Colloid Interface Sci.*, 1966, **22**, 462.
23 H. M. Princen, *J. Colloid Interface Sci.*, 1979, **71**, 55.
24 C. Solans, J. Esquena, N. Azemar, C. Rodríguez and H. Kunieda, in *Emulsions: Structure, Stability and Interactions*, ed. D. N. Petsev, Elsevier, Amsterdam, 2004.
25 V. H. Bartl and W. Von Bonin, *Macromol. Chem. Phys.*, 1962, **57**, 74.
26 D. Barby and Z. Haq, European patent, 0060138, 1982.
27 E. Ruckenstein and J. S. Park, *Polymer*, 1992, **33**, 405.
28 N. R. Cameron and D. C. Sherrington, *Adv. Polym. Sci.*, 1996, **126**, 162.
29 C. Solans, J. Esquena and N. Azemar, *Curr. Opin. Colloid Interface Sci.*, 2003, **8**, 156.
30 P. M. Claesson and B. W. Ninham, *Langmuir*, 1992, **8**, 1406.
31 E. Furusaki, Y. Ueno, N. Sakairi, N. Nishi and S. Tokura, *Carbohydr. Polym.*, 1996, **9**, 29.
32 M. Rinaudo, *Prog. Polym. Sci.*, 2006, **31**, 603.

33 M. Rinaudo, *Polym. Int.*, 2008, **57**, 397.
34 R. A. A. Muzzarelli, F. Greco, A. Busilacchi and V. Sollazzo, *Carbohydr. Polym.*, 2012, **89**, 723.
35 E. Agulló, R. Mato, C. Peniche, *et al.*, *Quitina y Quitosano: Obtención, caracterización y aplicaciones, Fondo Editorial de la Pontificia Universidad Católica del Perú*, Perú, 2004.
36 F. Shahidi, J. K. V. Arachchi and Y. J. Jeon, *Trends Food Sci. Technol.*, 1999, **10**, 37.
37 I. Y. Kim, S. J. Kim, M.-S. Shin, Y. M. Lee, D.-I. Shin and S. I. Kim, *J. Appl. Polym. Sci.*, 2002, **85**, 2661.
38 S. Chen, M. Liu, S. Jin and Y. Chen, *J. Appl. Polym. Sci.*, 2005, **98**, 1720.
39 L. Yin, L. Fei, F. Cui, C. Tang and C. Yin, *Biomaterials*, 2007, **28**, 1258.
40 C. Nishi, N. Nakajima and Y. Ikada, *J. Biomed. Mater. Res.*, 1995, **29**, 829.
41 P. C. Schulz, M. S. Rodríguez, L. F. Del Blanco, M. Pistonesi and E. Agulló, *Colloid Polym. Sci.*, 1998, **276**, 1159.
42 S. Mun, E. A. Decker and D. J. McClements, *Langmuir*, 2005, **21**, 6228.
43 N. Calero, J. Muñoz, P. W. Cox, A. Heuer and A. Guerrero, *Food Hydrocolloids*, 2013, **30**, 152.
44 Th. F. Tadros and B. Vincent, in *Encyclopedia of Emulsion Technology*, ed. P. Becher, Marcel Dekker, New York, 1983, ch. 3.
45 I. M. Lifshitz and V. V. Slyozov, *J. Phys. Chem. Solids*, 1961, **19**, 35.
46 C. Wagner, *Z. Elektochem.*, 1961, **65**, 581.
47 B. Deminiere, A. Colin, F. Leal Calderon and J. Bibette, Lifetime and destruction of concentrated emulsions undergoing coalescence, in *Modern Aspects of Emulsion Science*, ed. B. P. Binks, The Royal Society of Chemistry, Cambridge (UK), 1998, ch. 8, pp. 261–291.
48 E. G. Cockbain and T. S. McRoberts, *J. Colloid Sci.*, 1953, **8**, 440.
49 G. W. J. Lee and Th. F. Tadros, *Colloids Surf.*, 1982, **5**, 117.
50 Th. F. Tadros, Use of rheological measurements for assesment and prediction of the long-term physical stability of formulations, in *Rheology of dispersions: Principles and applications*, Wiley-VCH, Weinheim (Germany), 2010, ch. 8.
51 Th. F. Tadros, Emulsions Science and Technology: A General Introduction, in *Emulsion Science and Technology*, Wiley-VCH, Weinheim (Germany), 2009, ch. 1, pp. 18–19.
52 I. Pepić, J. Filipović and I. Jalšenjak, *Colloids Surf., A*, 2008, **327**, 95.
53 R. Pal, *AIChe J.*, 1996, **42**, 3181.
54 A. Langenfeld, V. Schmitt and M. J. Stébé, *J. Colloid Interface Sci.*, 1999, **218**, 522.
55 Th. F. Tadros, *Langmuir*, 1990, **6**, 28.
56 M. J. Moura, M. M. Figueiredo and M. H. Gil, *Biomacromolecules*, 2007, **8**, 3823.
57 P. Matricardi, M. Pontoriero, T. Coviello, M. A. Casadei and F. Alhaique, *Biomacromolecules*, 2008, **9**, 2014.
58 C. A. Bonino, J. E. Samorezov, O. Jeon, E. Alsberg and S. A. Khan, *Soft Matter*, 2011, **7**, 11510.
59 P. M. Gilsenan and S. B. Ross-Murphy, *Int. J. Biol. Macromol.*, 2001, **29**, 53.
60 E. Marsich, M. Borgogna, I. Donati, P. Mozetic, B. L. Strand, S. Gomez Salavador, F. Vittur and S. Paoletti, *J. Biomed. Mater. Res., Part A*, 2007, **84**, 364.

